BioChem

MDPI

Article

Isopanduratin A Inhibits Tumor Necrosis Factor (TNF)-α-Induced Nuclear Factor κB Signaling Pathway by Promoting Extracellular Signal-Regulated Kinase-Dependent Ectodomain Shedding of TNF Receptor 1 in Human Lung Adenocarcinoma A549 Cells

Chihiro Moriwaki [1], Riho Tanigaki [1], Yasunobu Miyake [2], Nghia Trong Vo [1], Mai Thanh Thi Nguyen [3,4,5], Nhan Trung Nguyen [3,4,5], Truong Nhat Van Do [3,4,5], Hai Xuan Nguyen [3,4,5] and Takao Kataoka [1,6,*]

1 Department of Applied Biology, Kyoto Institute of Technology, Matsugasaki, Sakyo-ku, Kyoto 606-8585, Japan; chihiro.moriwaki@gmail.com (C.M.); tngk.mameuma@gmail.com (R.T.); votrongnghia258@gmail.com (N.T.V.)
2 Division of Molecular and Cellular Immunoscience, Department of Biomolecular Sciences, Faculty of Medicine, Saga University, Saga 849-8501, Japan; ymiyake@cc.saga-u.ac.jp
3 Faculty of Chemistry, University of Science, 227 Nguyen Van Cu Street, District 5, Ho Chi Minh City 72711, Vietnam; nttmai@hcmus.edu.vn (M.T.T.N.); ntnhan@hcmus.edu.vn (N.T.N.); dvntruong@hcmus.edu.vn (T.N.V.D.); nxhai@hcmus.edu.vn (H.X.N.)
4 Cancer Research Laboratory, University of Science, 227 Nguyen Van Cu Street, District 5, Ho Chi Minh City 72711, Vietnam
5 Linh Trung Ward, Vietnam National University, Ho Chi Minh City 71300, Vietnam
6 The Center for Advanced Insect Research Promotion (CAIRP), Kyoto Institute of Technology, Matsugasaki, Sakyo-ku, Kyoto 606-8585, Japan
* Correspondence: takao.kataoka@kit.ac.jp

Citation: Moriwaki, C.; Tanigaki, R.; Miyake, Y.; Vo, N.T.; Nguyen, M.T.T.; Nguyen, N.T.; Do, T.N.V.; Nguyen, H.X.; Kataoka, T. Isopanduratin A Inhibits Tumor Necrosis Factor (TNF)-α-Induced Nuclear Factor κB Signaling Pathway by Promoting Extracellular Signal-Regulated Kinase-Dependent Ectodomain Shedding of TNF Receptor 1 in Human Lung Adenocarcinoma A549 Cells. *BioChem* **2021**, *1*, 174–189. https://doi.org/10.3390/biochem1030014

Academic Editor: Yehia Mechref

Received: 30 July 2021
Accepted: 22 October 2021
Published: 1 November 2021

Abstract: Tumor necrosis factor α (TNF-α) induces the nuclear factor κB (NF-κB) signaling pathway via TNF receptor 1 (TNF-R1). We recently reported that isopanduratin A inhibited the TNF-α-induced NF-κB signaling pathway in human lung adenocarcinoma A549 cells. In the present study, we found that isopanduratin A did not inhibit the interleukin-1α-induced NF-κB signaling pathway in A549 cells. Isopanduratin A down-regulated the expression of TNF-R1 in these cells. We also revealed that isopanduratin A down-regulated the cell surface expression of TNF-R1 by promoting the cleavage of TNF-R1 into its soluble forms. TAPI-2, an inhibitor of TNF-α-converting enzyme, suppressed the inhibitory activity of isopanduratin A against the TNF-α-induced activation of NF-κB. The mitogen-activated protein (MAP) kinase/extracellular signal-regulated kinase (ERK) kinase inhibitor U0126, but not the p38 MAP kinase inhibitor SB203580, blocked the ectodomain shedding of TNF-R1 induced by isopanduratin A. Consistent with this result, isopanduratin A induced the rapid phosphorylation of ERK, but not p38 MAP kinase. Isopanduratin A also promoted the phosphorylation of eukaryotic initiation factor 2α (eIF2α). The present results indicate that isopanduratin A inhibits TNF-α-induced NF-κB signaling pathway by promoting ERK-dependent ectodomain shedding of cell surface TNF-R1, and also decreases cellular TNF-R1 levels through the phosphorylation of eIF2α in A549 cells.

Keywords: isopanduratin A; tumor necrosis factor receptor 1; extracellular signal-regulated kinase; eukaryotic initiation factor 2α; ectodomain shedding

1. Introduction

Inflammatory cytokines, such as tumor necrosis factor α (TNF-α), are produced by activated macrophages, and stimulate other types of cells to provoke inflammatory responses [1]. TNF-α induces intracellular signaling pathways, one of which leads to the activation of the transcription factor nuclear factor κB (NF-κB) [2,3]. Upon engaging with TNF-α, TNF receptor 1 (TNF-R1) recruits adaptor proteins to form a membrane-proximal

complex, which is required for the activation of inhibitor of NF-κB (IκB) kinase [2,3]. IκBα is associated with NF-κB subunits in the cytosol and is rapidly phosphorylated by IκB kinase in response to a TNF-α stimulation, leading to its ubiquitination and degradation by proteasomes [4,5]. NF-κB subunits, typically composed of RelA (also known as p65) and p50, translocate to the nucleus and activate many of the genes that are essential for inflammatory responses [6,7].

The metalloproteinase TNF-α-converting enzyme (TACE) (also known as ADAM17) mediates ectodomain shedding by cleaving the membrane-bound forms of TNF-α to its soluble forms and plays an essential role under physiological and pathological conditions [8,9]. In addition to TNF-α, TACE is able to cleave other ligands and receptors, including TNF-R1 [9]. TACE possesses the C-terminal cytoplasmic domain that regulates the catalytic activity of its extracellular domain [9]. TACE activity is up-regulated via the phosphorylation of Thr 735 by extracellular signal-regulated kinase (ERK) and p38 mitogen-activated protein (MAP) kinase [10–13]. Particular types of translation inhibitors (e.g., anisomycin, glutarimides, and triene-ansamycins) induce the activation of ERK and p38 MAP kinase via a ribotoxic stress response [14,15]. We previously reported that translation inhibitors (e.g., acetoxycycloheximide, cytotrienin A, deoxynivalenol, and irciniastatin A) promoted TACE-dependent TNF-R1 ectodomain shedding by activating ERK and p38 MAP kinase [16–21].

Panduratins are characterized by cyclohexene chalcones and belong to a family of flavonoids [22]. Panduratin derivatives have been reported to exert diverse biological effects, including anti-cancer and anti-inflammatory activities [22–25]. Isopanduratin A has been shown to exhibit anti-bacterial activity against *Streptococcus mutans* and acne-causing microorganisms [26,27], inhibitory activities toward melanin biosynthesis and tyrosinase [28], suppressive effects on TNF-α-induced cytotoxicity and aminopeptidase N [29], and α-glucosidase and pancreatic lipase inhibitory activities [30]. We previously identified eight new cyclohexene chalcones and seven known compounds, including isopanduratin A, in the rhizome extracts of *Boesenbergia pandurata*, a medicinal plant belonging to the Zingiberaceae family, as agents that exhibited potent cytotoxic activities in the human pancreatic cancer line PANC-1 [31]. Consistent with previous findings [32], we showed that isopanduratin A exhibited anti-cancer activity towards PANC-1 and the human hepatocellular carcinoma cell line HepG2 [31,33]. In addition to these anti-cancer activities, we recently reported that isopanduratin A inhibited the TNF-α-induced NF-κB-dependent signaling pathway in the human lung adenocarcinoma cell line A549 [34]. 4-Hydroxypanduratin A has also been shown to inhibit the TNF-α-induced NF-κB-dependent signaling pathway [34]. Consistent with our studies, panduratin A and its derivatives inhibited the NF-κB signaling pathway in different cell lines [35–38]. However, the molecular targets of panduratin derivatives in the NF-κB signaling pathway remain unclear. In the present study, we elucidated the mechanisms by which isopanduratin A inhibited the TNF-α-induced NF-κB signaling pathway.

2. Materials and Methods

2.1. Cell Culture

A549 cells (JCRB0076) were obtained from the National Institutes of Biomedical Innovation, Health, and Nutrition JCRB Cell Bank (Osaka, Japan) and maintained in RPMI 1640 medium (Thermo Fisher Scientific, Waltham, MA, USA) supplemented with heat-inactivated fetal calf serum (Sigma-Aldrich, St. Louis, MO, USA) and penicillin-streptomycin mixed solution (Nacalai Tesque, Kyoto, Japan) as previously described [39,40]. RPMI 1640 medium without fetal calf serum was used in experiments to examine the phosphorylation of ERK, p38 MAP kinase, and c-Jun N-terminal kinase (JNK).

2.2. Reagents

(±)-Isopanduratin A (Figure 1A) was purified from the methanol extract of rhizomes of *B. pandurata* as previously described [31]. Deoxynivalenol (Sigma-Aldrich, St. Louis, MO,

USA), SB253080 (Cayman Chemical, Ann Arbor, MI, USA), SP600125 (Sigma-Aldrich), TNF-α protease inhibitor-2 (TAPI-2) (Peptide Institute, Osaka, Japan), and U0126 (Wako Pure Chemical Industries, Osaka, Japan) were commercially obtained. TNF-α and interleukin (IL)-1α were provided by Dainippon Pharmaceuticals (Osaka, Japan).

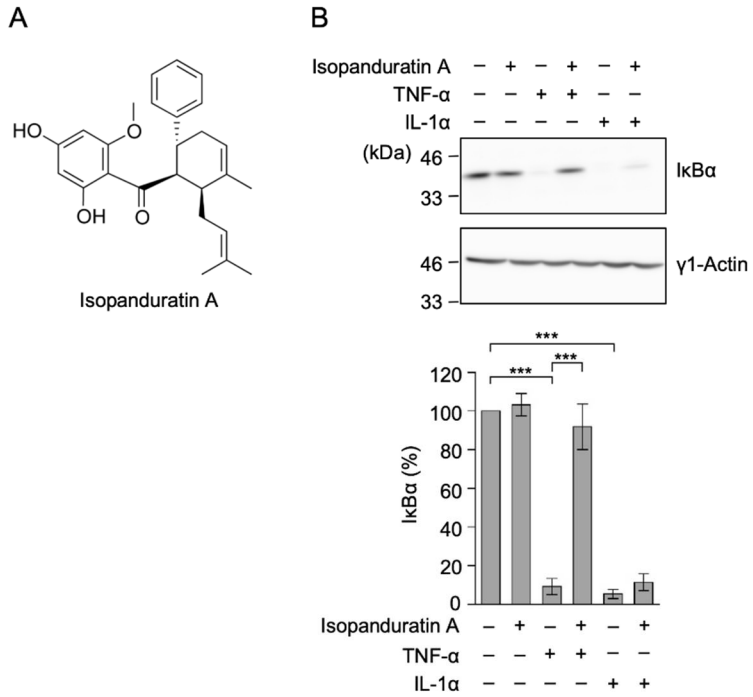

Figure 1. Isopanduratin A inhibited IκBα degradation induced by TNF-α, but not IL-1α. (**A**) Structure of isopanduratin A. (**B**) A549 cells were treated with (+) or without (−) isopanduratin A for 1 h, and then stimulated with (+) TNF-α (2.5 ng/mL) or IL-1α (0.25 ng/mL) or without cytokines (−) for 15 min in the presence or absence of isopanduratin A (50 μM). Cell lysates were analyzed by Western blotting. IκBα (%) is shown as the mean ± S.E. of three independent experiments. *** $p < 0.001$.

2.3. Antibodies

Primary antibodies reactive to β-actin (AC-15; Sigma-Aldrich), γ1-actin (2F3; Wako Pure Chemical Industries), ERK (137F5; Cell Signaling Technology, Danvers, MA, USA), eukaryotic initiation factor 2α (eIF2α) (D7D3; Cell Signaling Technology), FLAG (1E6; Wako Pure Chemical Industries), glyceraldehyde-3-phosphophate dehydrogenase (GAPDH) (6C5; Santa Cruz Biotechnology, Dallas, TX, USA), IκBα (25; BD Biosciences, San Jose, CA, USA), JNK (#9252; Cell Signaling Technology), lamin A/C (E-1; Santa Cruz Biotechnology), p38 MAP kinase (#9212; Cell Signaling Technology), phospho-eIF2α (Ser51) (D9G8; Cell Signaling Technology), phospho-ERK (Thr202/Tyr204) (#9101; Cell Signaling Technology), phospho-JNK (Thr183/Tyr185) (#9251; Cell Signaling Technology), phospho-p38 MAP kinase (Thr180/Tyr182) (D3F9; Cell Signaling Technology), RelA (C-20; Santa Cruz Biotechnology), TNF-R1 (H-5; Santa Cruz Biotechnology), TNF-R1 (16803; R&D Systems, Minneapolis, MN, USA), and the mouse IgG1 isotype control (MOPC-21; BioLegend, Sand Diego, CA, USA) were used in experiments. γ1-Actin and β-actin were expressed similarly in A549 cells.

2.4. Western Blotting

Cells were washed with phosphate-buffered saline (PBS) and then lysed with Triton X-100 lysis buffer containing the protease inhibitor cocktail cOmplete™ (Sigma-Aldrich) and phosphatase inhibitor cocktail (Nacalai Tesque). Nuclear and cytoplasmic fractions were prepared as reported in previous studies [19,41]. Cell lysates were centrifuged (15,300× *g*, 5 min) and separated into supernatants (cytoplasmic fractions) and pellets. The pellets

were washed with Triton X-100 lysis buffer, sonicated, and collected as nuclear fractions. The culture medium was processed to precipitate proteins by chloroform/methanol as previously described [16,19]. Western blotting was performed according to a previously described method [39,40]. Proteins were separated by SDS-polyacrylamide gel electrophoresis and transferred to nitrocellulose membranes, followed by blocking with skimmed milk. Membranes were then reacted serially with primary antibodies and peroxidase-conjugated anti-mouse IgG or anti-rabbit IgG antibodies (Jackson ImmunoResearch, West Grove, PA, USA), and subjected to a chemiluminescence reaction. Blots were analyzed by ImageQuant LAS 4000 mini (GE Healthcare Japan, Tokyo, Japan) and Amersham Imager 680 (GE Healthcare Japan).

2.5. Transfection

The pCR3 expression vector encoding C-terminal FLAG-tagged human full-length TNF-R1 was previously described [42]. A549 cells were transfected with the pCR3 expression vector encoding TNF-R1-FLAG by the lipofection method using HilyMax transfection reagent (Dojindo, Kumamoto, Japan). Transfected A549 cells were then treated with compounds.

2.6. Flow Cytometry

Cells were harvested and then stained with either an anti-TNF-R1 antibody (16803) or an isotype control antibody (MOPC-21). Cells were washed and stained with a phycoerythrin-labeled anti-mouse IgG antibody (Jackson ImmunoResearch). Flow cytometric analysis was performed using FACSCalibur (BD Biosciences) as previously described [43]. Data were analyzed by FlowJo software (Tomy Digital Biology, Tokyo, Japan).

2.7. Statistical Analysis

Data were analyzed by a one-way ANOVA and Tukey's post-hoc test for multiple comparisons.

3. Results

3.1. Isopanduratin A Inhibited IκB Degradation Induced by TNF-α, but Not IL-1α

In NF-κB signaling pathways, TNF-α and IL-1α induce the formation of different membrane-proximal complexes, which converge to activate IκB kinases as the main target [2,3]. To clarify whether isopanduratin A inhibits the converged NF-κB signaling pathway, A549 cells were pretreated with isopanduratin A, followed by TNF-α or IL-1α. Consistent with our previous findings [34], isopanduratin A inhibited IκBα degradation induced by TNF-α (Figure 1B). By contrast, IκBα degradation induced by IL-1α was not inhibited by isopanduratin A (Figure 1B). These results indicated that isopanduratin A selectively inhibited the early NF-κB signaling pathway induced by TNF-α in A549 cells.

3.2. Isopanduratin A Decreased the Expression of TNF-R1

A549 cells have been shown to express TNF-R1, but not TNF-R2 [16]. We investigated the expression of TNF-R1 at the protein level by Western blotting. The treatment with isopanduratin A for 1 h markedly decreased bands reactive to the anti-TNF-R1 monoclonal antibody (clone H-5) in a dose-dependent manner (Figure 2A). Allantopyrone A is a natural metabolite produced by the endophytic fungus *Allantophomopsis lycopodiana* KS-97 and contains two α,β-unsaturated carbonyl moieties [44], which are reactive to cysteinyl thiol groups. We previously showed that allantopyrone A, which directly bound to TNF-R1, possibly via cysteine residues, reduced the TNF-R1 reactivity of H-5, which appeared to decrease TNF-R1 bands on Western blots [42]. To exclude this possibility, we transfected A549 cells with an expression vector encoding C-terminal FLAG-tagged TNF-R1. Isopanduratin A also decreased the expression of TNF-R1-FLAG in a dose-dependent manner (Figure 2B). Collectively, these results indicated that isopanduratin A reduced the amount of TNF-R1 in A549 cells.

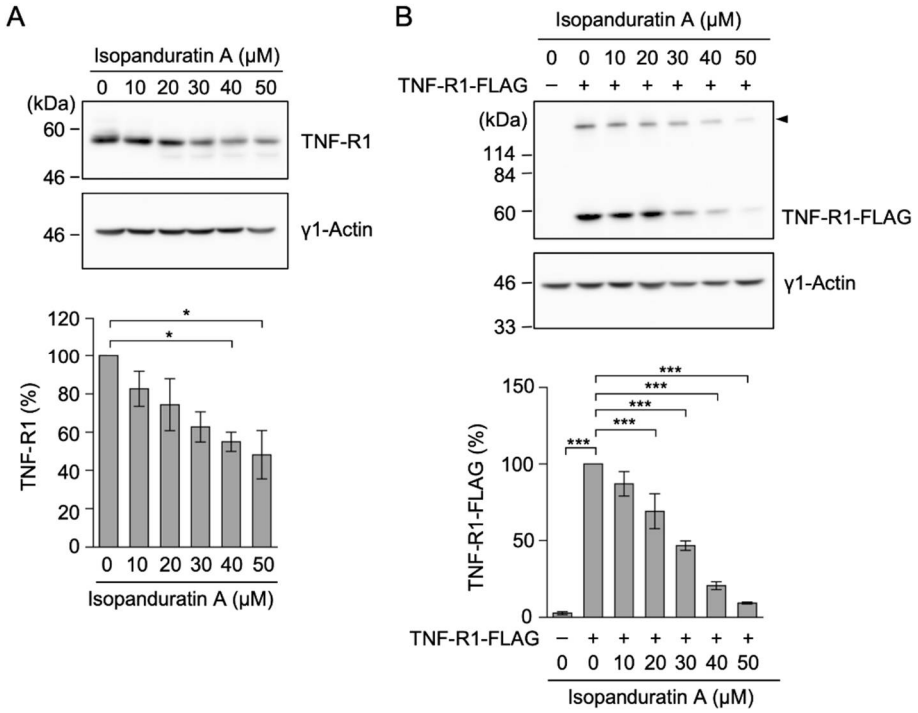

Figure 2. Isopanduratin A decreased the amount of TNF-R1. (**A**) A549 cells were treated with the indicated concentrations of isopanduratin A for 1 h. Cell lysates were analyzed by Western blotting. The amount of TNF-R1 in non-treated A549 cells is set to 100%. TNF-R1 (%) is shown as the mean ± S.E. of three independent experiments. * $p < 0.05$. (**B**) A549 cells were transfected with (+) or without (−) an expression vector encoding TNF-R1-FLAG, and then treated with the indicated concentrations of isopanduratin A for 1 h. The arrowhead indicates the high molecular weight band of transfected TNF-R1-FLAG, which may form homotrimers under reducing conditions [42]. TNF-R1-FLAG (%) is shown as the mean ± S.E. of three independent experiments. *** $p < 0.001$.

3.3. Isopanduratin A Induced the Ectodomain Shedding of TNF-R1

TACE has the ability to cleave membrane-bound TNF-R1, and its soluble form is released into culture medium [8,9]. The time-course experiment showed that soluble TNF-R1 was steadily augmented 40–60 min after the exposure to isopanduratin A (Figure 3A). The amount of membrane-bound TNF-R1 in the cell lysate was conversely decreased by isopanduratin A (Figure 3A). TAPI-2, *N*-(*R*)-[2-(hydroxyaminocarbonyl)methyl]-4-methypentanoyl-L-*t*-butyl-alanyl-L-analnine, 2-aminoethyl amide, is a small molecule inhibitor of TACE. TAPI-2 has been shown to block the TACE-dependent cleavage of TNF-R1 in A549 cells [16,18–20]. TAPI-2 decreased the augmentation of soluble TNF-R1 in isopanduratin A-treated A549 cells (Figure 3B). In contrast, TAPI-2 did not markedly restore the decreased amount of membrane-bound TNF-R1 in the cell lysate of isopanduratin A-treated cells (Figure 3B). These results indicated that isopanduratin A induced the TACE-dependent cleavage of membrane-bound TNF-R1 into its soluble form. An additional TACE-independent mechanism was also suggested to be responsible for the reduction induced in membrane-bound TNF-R1 in the cell lysate by isopanduratin A.

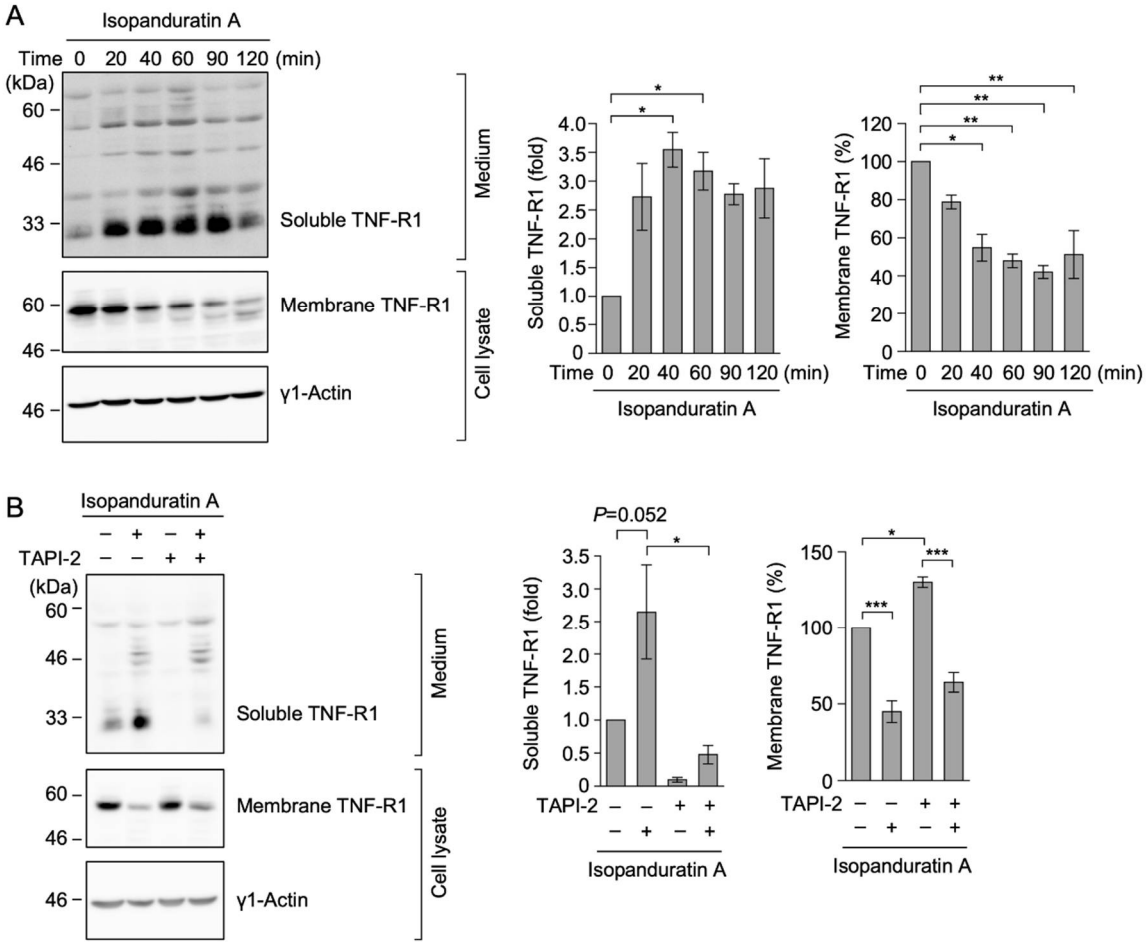

Figure 3. Isopanduratin A induced the ectodomain shedding of TNF-R1 by TACE. (**A**) A549 cells were treated with isopanduratin A (30 μM) for the indicated times. (**B**) A549 cells were pretreated with (+) or without (−) TAPI-2 for 1 h, and were then treated with (+) or without (−) isopanduratin A. Final concentrations used: isopanduratin A (50 μM) and TAPI-2 (25 μM). Cell lysates and culture medium were analyzed by Western blotting. The amount of TNF-R1 was normalized to that of γ1-actin. The amounts of soluble TNF-R1 and membrane TNF-R1 in control A549 cells were set to 1-fold and 100%, respectively. Soluble TNF-R1 (fold) in medium and membrane TNF-R1 (%) in cell lysates are shown as the mean ± S.E. of three independent experiments. * $p < 0.05$, ** $p < 0.01$, and *** $p < 0.001$.

We then evaluated the cell surface expression of TNF-R1 by flow cytometry. In comparison with the control (Figure 4Aa), isopanduratin A markedly decreased the expression of cell surface TNF-R1 (Figure 4Ab). TAPI-2 alone up-regulated the expression of cell surface TNF-R1 (Figure 4Ac), suggesting that TNF-R1 was constitutively processed by TACE. TAPI-2 reversed the expression of cell surface TNF-R1 in isopanduratin A-treated A549 cells (Figure 4Ad). These results were confirmed by the quantitation of cell surface TNF-R1 (Figure 4B). These results clearly indicated that isopanduratin A induced the ectodomain shedding of TNF-R1.

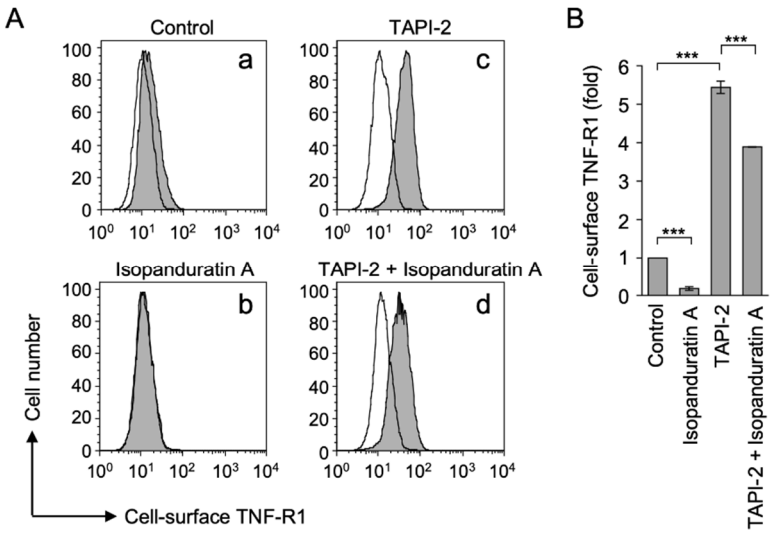

Figure 4. Isopanduratin A diminished the expression of cell surface TNF-R1. (**A**,**B**) A549 cells were treated with or without TAPI-2 for 1 h, and further incubated with or without isopanduratin A (50 μM) and TAPI-2 (25 μM) for 1 h. The cell surface expression of TNF-R1 was measured by flow cytometry. Histograms are representative of three independent experiments (**A**). Upper left: control (**a**); lower left: isopanduratin A (**b**); upper right: TAPI-2 (**c**), and lower right: TAPI-2 + isopanduratin A (**d**). The amount of cell surface TNF-R1 in control A549 cells was set to 1-fold. Cell surface TNF-R1 (fold) is shown as the mean ± S.E. of three independent experiments (**B**). *** $p < 0.001$.

3.4. Isopanduratin A Inhibited the TNF-α-Induced NF-κB Signaling Pathway by Inducing the Ectodomain Shedding of TNF-R1

Consistent with our previous findings [34], isopanduratin A inhibited the nuclear translocation of RelA in A549 cells stimulated with TNF-α (Figure 5A, Lanes 3 and 4). The pretreatment with TAPI-2 markedly suppressed the isopanduratin A-induced inhibition of the nuclear translocation of RelA (Figure 5A, Lanes 4 and 6). TAPI-2 also restored TNF-α-induced IκBα degradation in isopanduratin A-treated A549 cells (Figure 5B, Lanes 4 and 6). These results indicated that isopanduratin A inhibited the TNF-α-induced the NF-κB signaling pathway by inducing the ectodomain shedding of TNF-R1.

3.5. Isopanduratin A Induced the Ectodomain Shedding of TNF-R1 by ERK Activation

The catalytic activity of TACE was previously shown to be activated by the phosphorylation of the Thr 735 residue in its cytoplasmic tail by ERK and p38 MAP kinase [10–13]. To elucidate the involvement of ERK and/or p38 MAP kinase, A549 cells were pretreated with these kinase inhibitors, followed by isopanduratin A. The MAP kinase/ERK kinase (MEK) inhibitor U0126 diminished the amount of soluble TNF-R1 in the culture medium of isopanduratin A-treated A549 cells (Figure 6, Lane 3). In contrast, the p38 MAP kinase inhibitor SB203580 and the JNK inhibitor SP600125 did not markedly affect the augmentation of soluble TNF-R1 in isopanduratin A-treated A549 cells (Figure 6, Lanes 4 and 5). The decrease observed in membrane-bound TNF-R1 in the cell lysate by isopanduratin A was not markedly reversed by U0126 (Figure 6, Lane 3). These results clearly indicated that isopanduratin A induced the ERK-dependent ectodomain shedding of TNF-R1.

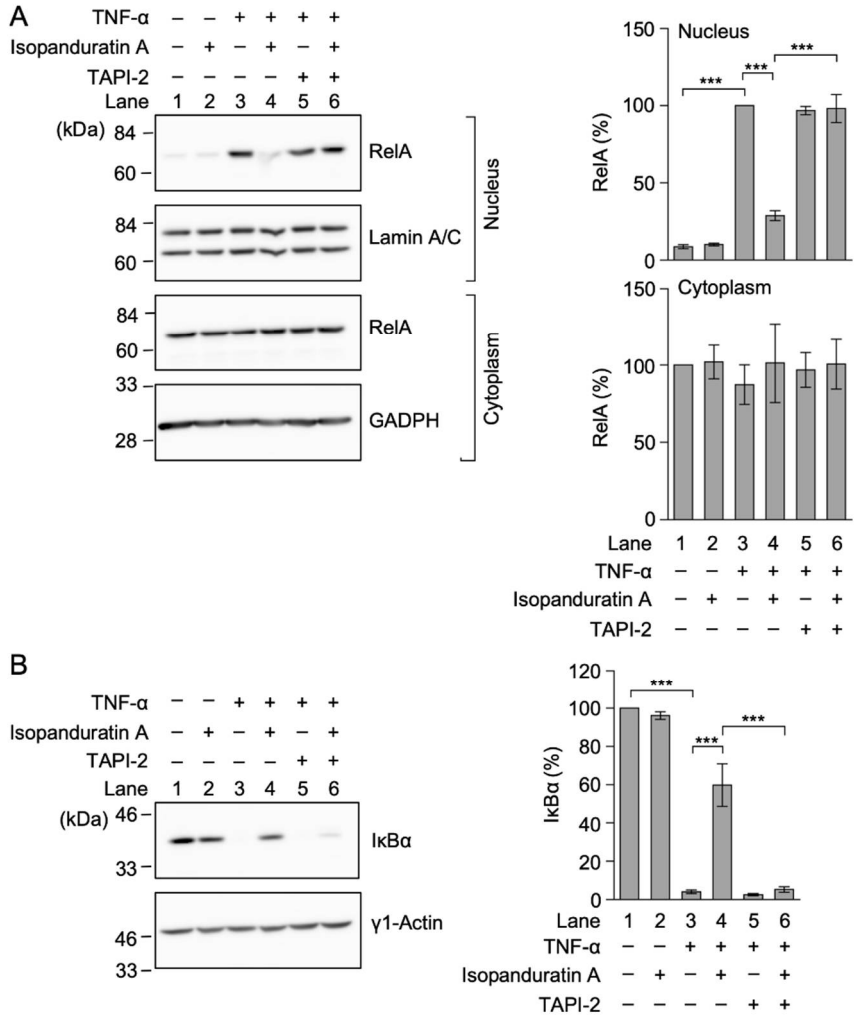

Figure 5. TAPI-2 reversed the inhibition of the TNF-α-induced NF-κB signaling pathway by isopanduratin A. (**A**,**B**) A549 cells were treated with (+) or without (−) TAPI-2 for 1 h, then incubated with (+) or without (−) isopanduratin A for 1 h, followed by a stimulation with (+) or without (−) TNF-α (2.5 ng/mL) for 15 min (**B**) and 30 min (**A**) in the presence or absence of isopanduratin A (50 μM) and TAPI-2 (25 μM). Cytoplasmic and nuclear fractions were prepared and analyzed by Western blotting. The amounts of RelA in the nucleus of TNF-α-stimulated A549 cells and RelA in the cytoplasm of control A549 cells are set to 100%. RelA (%) in the nucleus and RelA (%) in the cytoplasm are shown as the mean ± S.E. of three independent experiments. The amount of IκBα was normalized to that of γ1-actin. The amount of IκBα in control A549 cells was set to 100%. IκBα (%) is shown as the mean ± S.E. of three independent experiments. *** $p < 0.001$.

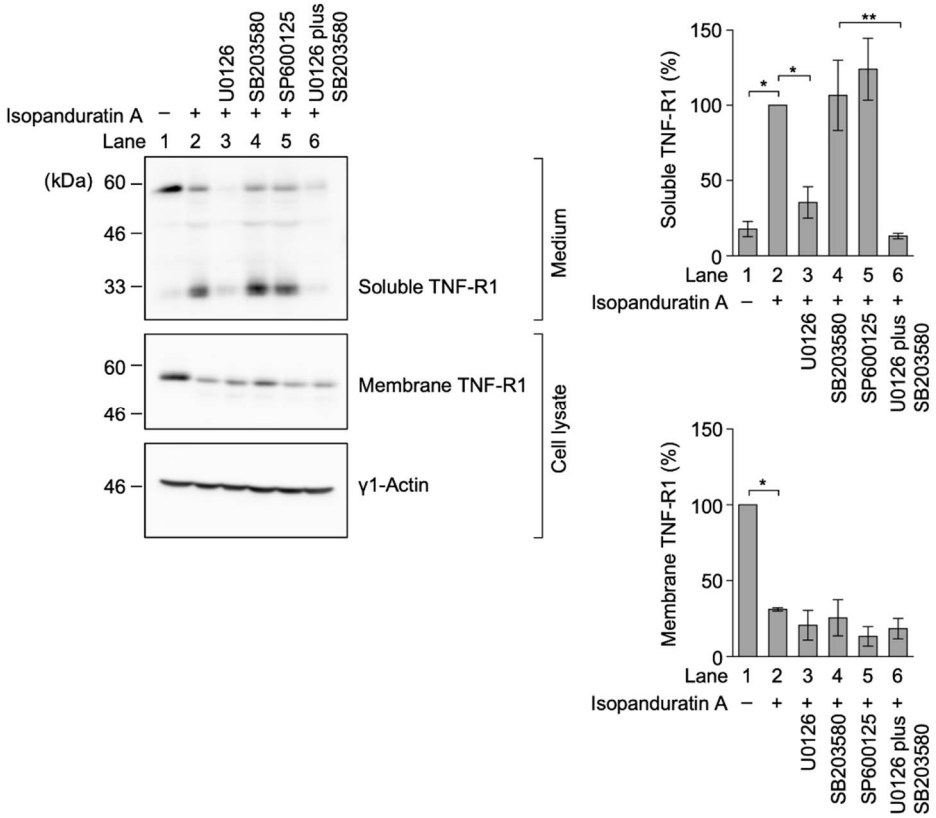

Figure 6. U0126 inhibited the ectodomain shedding of TNF-R1 induced by isopanduratin A. A549 cells were treated with or without U0126, SB203580, SP600125, or U0126 plus SB203580 for 1 h, and incubated with (+) or without (−) isopanduratin A (50 μM) for 1 h in the presence or absence of U0126, SB203580, SP600125, or U0126 plus SB203580 (each 10 μM). Cell lysates and culture medium were analyzed by Western blotting. The amount of TNF-R1 in cell lysates was normalized to that of γ1-actin. The amounts of soluble TNF-R1 in isopanduratin A-treated A549 cells and membrane TNF-R1 in control A549 cells were set to 100%. Soluble TNF-R1 (%) in medium and membrane TNF-R1 (%) in cell lysates are shown as the mean ± S.E. of three independent experiments. * $p < 0.05$ and ** $p < 0.01$.

3.6. Isopanduratin A Induced the Rapid Phosphorylation of ERK, but Not p38 MAP Kinase or JNK

We investigated whether isopanduratin A induced the activation of ERK, p38 MAP kinase, and JNK. Deoxynivalenol, a translation inhibitor, was used as a positive control because it was previously shown to promote the phosphorylation of ERK, p38 MAP kinase, and JNK in A549 cells [19,21]. Consistent with these findings, phosphorylated bands of ERK, p38 MAP kinase, and JNK were clearly detectable in deoxynivalenol-treated A549 cells (Figure 7B). In contrast, the phosphorylation of ERK was augmented by isopanduratin A within 20 min and maintained for up to 120 min, while it induced the phosphorylation of p38 MAP kinase and JNK and at later time points (Figure 7A). These results indicate that isopanduratin A induced the rapid phosphorylation of ERK.

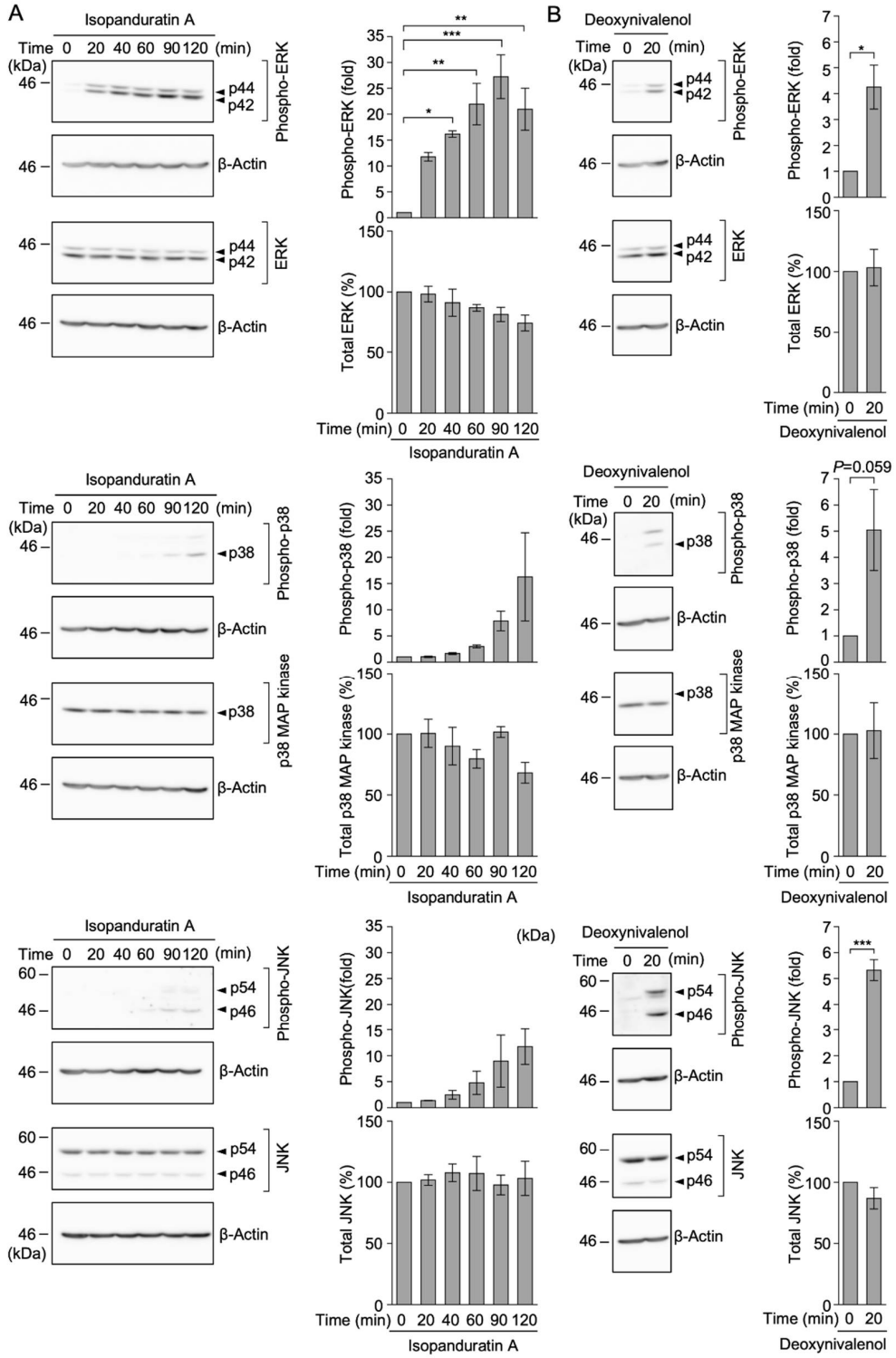

Figure 7. Isopanduratin A induced the rapid phosphorylation of ERK. (**A**,**B**) A549 cells were incubated with isopanduratin A (50 μM) (**A**) or deoxynivalenol (10 μM) (**B**) for the indicated times. Cell lysates were analyzed by Western blotting. The amounts of phospho-ERK, total ERK, phospho-p38 MAP kinase, total p38 MAP kinase, phospho-JNK, and total JNK were normalized to that of β-actin. The amounts of phospho-ERK, phospho-p38 MAP kinase, and phospho-JNK in control A549 cells are set to 1-fold. The amounts of total ERK, total p38 MAP kinase, and total JNK in control A549 cells are set to 100%. Phospho-ERK (fold), phospho-p38 MAP kinase (fold) phospho-JNK (fold), total ERK (%), total p38 MAP kinase (%), and total JNK (%) are shown as the mean ± S.E. of three independent experiments. * $p < 0.05$, ** $p < 0.01$, and *** $p < 0.001$.

We also investigated the selectivity of protein kinase inhibitors on ERK phosphorylation. The isopanduratin A-induced phosphorylation of ERK in A549 cells was markedly reduced by U0126 or U0126 plus SB203580 (Figure 8, Lanes 3 and 6), while it was barely affected by SB203580 or SP600125 (Figure 8, Lanes 4 and 5). These results confirmed that U0126 inhibited the isopanduratin A-induced activation of ERK.

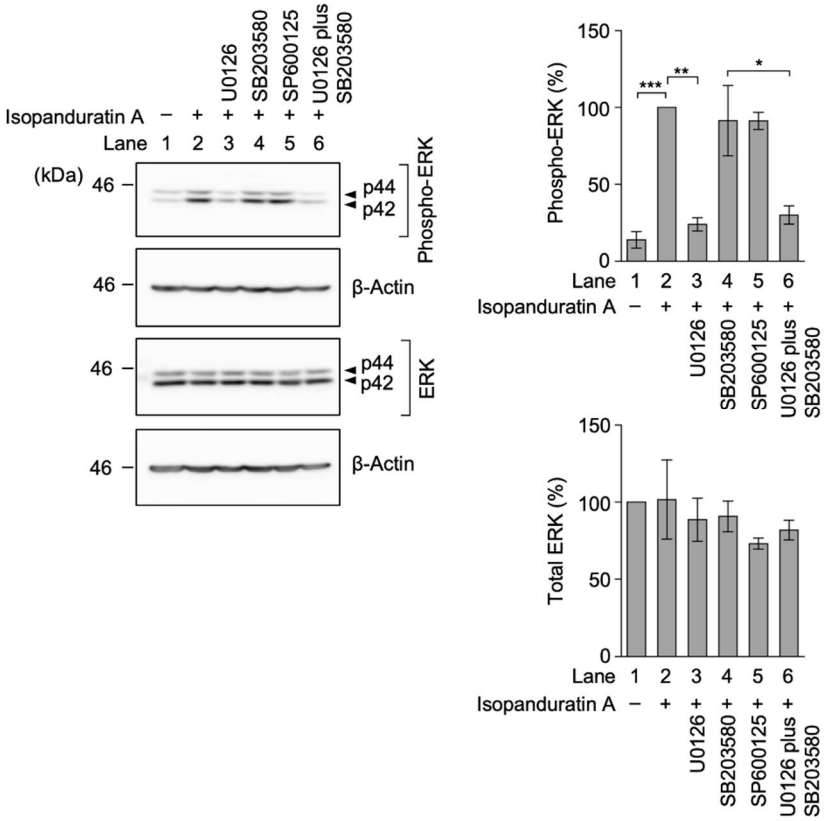

Figure 8. U0126 inhibited ERK phosphorylation induced by isopanduratin A. A549 cells were treated with or without U0126, SB203580, SP600125, or U0126 plus SB203580 for 1 h, and incubated with (+) or without (−) isopanduratin A (50 μM) for 1 h in the presence or absence of U0126, SB203580, SP600125, or U0126 plus SB203580 (10 μM each). Cell lysates were analyzed by Western blotting. The amounts of phospho-ERK and total ERK were normalized to that of β-actin. The amounts of phospho-ERK in isopanduratin A-treated A549 cells and total ERK in control A549 cells were set to 100%. Phospho-ERK (%) and total ERK (%) are shown as the mean ± S.E. of three independent experiments. * $p < 0.05$, ** $p < 0.01$, and *** $p < 0.001$.

3.7. Isopanduratin A Promoted eIF2α Phosphorylation

The inhibition of the ectodomain shedding of TNF-R1 by TAPI-2 or U0126 efficiently rescued the TNF-α-induced NF-κB signaling pathway, while it did not reverse the decrease in TNF-R1 in isopanduratin A-treated A549 cells (Figures 3B and 6). These data suggested that TNF-R1 is down-regulated in a manner independent of ectodomain shedding in isopanduratin A-treated A549 cells. eIF2 plays an essential role in the transport and entry of Met-tRNA$_i^{Met}$ to the ribosome small subunit during the initiation of translation [45,46]. The initiation step of translation is inhibited by Ser51 phosphorylation of the α subunit of eIF2 [45,46]. We found that isopanduratin A augmented the phosphorylation of eIF2α in a dose-dependent manner (Figure 9). In contrast, isopanduratin A did not affect the cellular level of eIF2α under the same conditions (Figure 9). These results indicated that isopanduratin A promoted eIF2α phosphorylation.

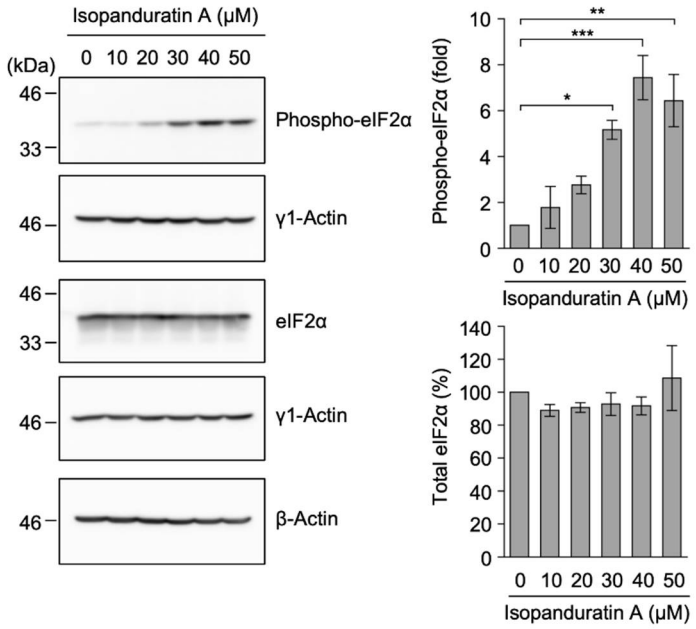

Figure 9. Isopanduratin A promoted eIF2α phosphorylation. A549 cells were treated with the indicated concentrations of isopanduratin A for 1 h. Cell lysates were analyzed by Western blotting. The amounts of phospho-eIF2α and total eIF2α were normalized to that of γ1-actin. The amounts of phospho-eIF2α and total eIF2α are set to 1-fold and 100%, respectively. Phospho-eIF2α (fold) and total eIF2α (%) are shown as the mean ± S.E. of three independent experiments. * $p < 0.05$, ** $p < 0.01$, and *** $p < 0.001$.

4. Discussion

Panduratin derivatives have been shown to exhibit anti-cancer activity through the induction of apoptosis and cell cycle arrest [36,47,48]. Panduratin derivatives have also been reported to exert anti-inflammatory effects [35–38]. Consistent with these findings, we previously showed that isopanduratin A inhibited TNF-α-induced IκBα phosphorylation and subsequent degradation at the early NF-κB signaling pathway in A549 cells [34]. The present results demonstrated that isopanduratin A selectively induced the ectodomain shedding of TNF-R1 via the ERK-dependent activation of TACE, thereby decreasing the cell surface expression of TNF-R1. Moreover, we showed that isopanduratin A did not affect IL-1α-induced IκBα degradation in A549 cells. These results clearly indicated that the inhibition of the TNF-α-induced NF-κB signaling pathway by isopanduratin A was due to a decrease in cell surface TNF-R1 expression and subsequent TNF-α unresponsiveness. Isopanduratin A also reduced the cellular amount of TNF-R1 by preventing translation via the phosphorylation of eIF2α. A schematic model for the biological activity of isopanduratin A on the ectodomain shedding of TNF-R1 and TNF-α-induced NF-κB activation is shown in Figure 10.

Panduratin A has been reported to inhibit the TNF-α-induced nuclear translocation of NF-κB subunits (i.e., RelA and p50) in A549 cells [36,37]. Panduratin A and isopanduratin A were also reported to inhibit TNF-α-induced cytotoxicity in L929 cells [29]. L929 cells undergo necroptosis in response to TNF-α [49]. In addition, panduratin A suppressed TNF-α-dependent muscle atrophy in rat skeletal muscle L6 cells [50]. Collectively, these findings indicated that panduratin A and isopanduratin A inhibited TNF-α-dependent cellular processes in different cell lines. This is consistent with our present result showing that isopanduratin A reduced TNF-α responsiveness by promoting the ectodomain shedding of TNF-R1 via TACE activity in A549 cells. TNF-R1 is mostly expressed in normal and transformed cells [51]. TACE is broadly expressed in various somatic tissues [8,52].

Therefore, it is conceivable that the cell surface expression of TNF-R1 is broadly regulated via TACE-dependent ectodomain shedding in various cell types.

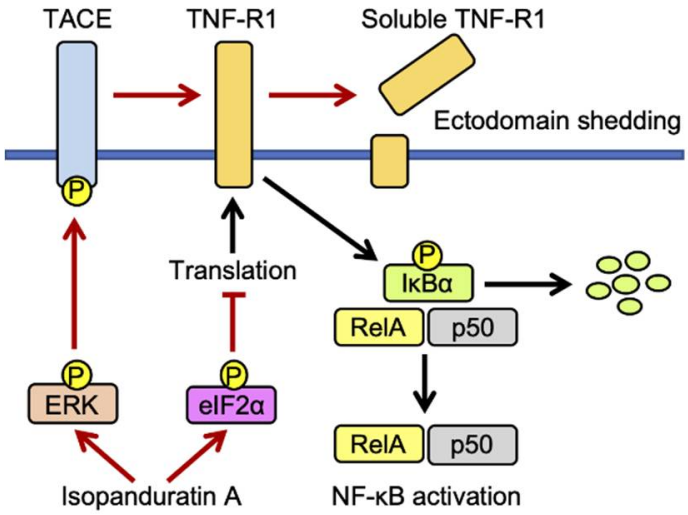

Figure 10. A schematic model for the biological activity of isopanduratin A. TACE plays a critical role in the ectodomain shedding of TNF-R1, and cleaves cell surface TNF-R1 into its soluble form. TACE is activated by the phosphorylation of its C-terminal cytoplasmic tail. Isopanduratin A induces the phosphorylation of ERK and eIF2α. Phosphorylated ERK mediates the phosphorylation and activation of TACE, which down-regulates cell surface TNF-R1 expression. In contrast, phosphorylated eIF2α blocks translation, thereby down-regulating cellular TNF-R1 expression. The NF-κB heterodimer composed of RelA and p50 is associated with IκBα in the cytosol. Upon engaging with TNF-α, IκBα is phosphorylated and undergoes ubiquitination and proteasomal degradation, leading to the liberation and subsequent nuclear translocation of RelA and p50. Isopanduratin A inhibits TNF-α-induced NF-κB activation by down-regulating cell surface TNF-R1 expression.

We showed that isopanduratin A promoted the ectodomain shedding of cell surface TNF-R1. Nevertheless, isopanduratin A still decreased the cellular amount of TNF-R1, even when A549 cells were treated together with TAPI-2 to block the cleavage and subsequent release of membrane-bound TNF-R1. These results suggested that isopanduratin A reduced the de novo protein synthesis of TNF-R1. The phosphorylation of eIF2α at Ser51 is well known to prevent a step in the initiation of translation and thereby block global protein synthesis [45,46]. eIF2α was phosphorylated in response to various cellular stresses [53,54]. We found that isopanduratin A up-regulated the level of phospho-eIF2α (Ser 51) within 1 h. Consistent with this, panduratin A has also been reported to up-regulate phospho-eIF2α (Ser51) in human malignant melanoma A375 cells for 24 h [55]. Therefore, panduratin derivatives appear to up-regulate eIF2α phosphorylation at least in different cell lines; however, their kinetics may differ between their structures and the cell types used.

Several translation inhibitors have the ability to induce the activation of MAP kinase superfamily members via a ribotoxic stress response mediated by ribosomes [14,15,56,57]. Among MAP kinase superfamily members, ERK and p38 MAP kinase phosphorylate the Thr 735 residue of TACE and activate its catalytic activity [10–13]. We previously showed that the ectodomain shedding of TNF-R1 was induced by acetoxycycloheximide, cytotrienin A, deoxynivalenol, and irciniastatin A [16–21]. We previously reported that the ectodomain shedding of TNF-R1 induced by three translation inhibitors (i.e., acetoxycycloheximide, cytotrienin A, or deoxynivalenol) was decreased to some extent by a single treatment with U0126 or SB203580, but was completely inhibited by a combined treatment of U0126 and SB203580 in A549 cells [17–19]. These studies reveal that ERK and p38 MAP kinase both play essential roles in the TACE-dependent TNF-R1 ectodomain shedding induced by those translation inhibitors in A549 cells. In contrast, the ectodomain shedding of TNF-R1

induced by irciniastatin A was inhibited by U0126, but not by SB203580, largely due to the fact that irciniastatin A induced activation of ERK, but not p38 MAP kinase in A549 cells [21]. These findings indicate that irciniastatin A uniquely induces TNF-R1 ectodomain shedding in a manner that is solely dependent on ERK. In this study, we showed that isopanduratin A promoted the ectodomain shedding of TNF-R1, which was sensitive to U0126, but not SB203580. Isopanduratin A induced the rapid activation of ERK, but not p38 MAP kinase. Thus, our present study reveals that isopanduratin A promotes the ERK-dependent ectodomain shedding of TNF-R1 and thereby inhibits the TNF-α-induced signaling pathway in A549 cells.

5. Conclusions

In conclusion, we revealed that isopanduratin A promoted the ectodomain shedding of TNF-R1 via the ERK-dependent activation of TACE. Moreover, isopanduratin A rapidly up-regulated the phosphorylation of eIF2α (Ser51). To date, panduratin derivatives have been shown to exert various biological effects, such as anti-cancer and anti-inflammatory activities. The present results showing that isopanduratin A is linked to ERK and eIF2α kinase provide insights into the mechanisms of actions of panduratin derivatives on various cellular activities.

Author Contributions: Conceptualization, C.M., R.T. and T.K.; formal analysis, C.M., R.T., Y.M., N.T.V. and T.K.; investigation, C.M., R.T., Y.M., N.T.V. and T.N.V.D.; resources, M.T.T.N., N.T.N., T.N.V.D. and H.X.N.; writing—original draft preparation, T.K.; writing—review and editing, Y.M. and T.K.; visualization, C.M., R.T. and T.K.; supervision, T.K.; funding acquisition, T.K. All authors have read and agreed to the published version of the manuscript.

Funding: This work was partly supported by the Japan Society for the Promotion of Science (JSPS) KAKENHI Grant number 19H02885 (to T.K.).

Institutional Review Board Statement: Not applicable.

Informed Consent Statement: Not applicable.

Data Availability Statement: The data presented in the present study are available upon request from the corresponding author.

Conflicts of Interest: The authors declare no conflict of interest.

References

1. Shapouri-Moghaddam, A.; Mohammadian, S.; Vazini, H.; Taghadosi, M.; Esmaeili, S.-A.; Mardani, F.; Seifi, B.; Mohammadi, A.; Afshari, J.T.; Sahebkar, A. Macrophage plasticity, polarization, and function in health and disease. *J. Cell Physiol.* **2018**, *233*, 6425–6440. [CrossRef]
2. Wajant, H.; Scheurich, P. TNFR1-induced activation of the classical NF-κB pathway. *FEBS J.* **2011**, *278*, 862–876. [CrossRef]
3. Hayden, M.S.; Ghosh, S. Regulation of NF-κB by TNF family cytokines. *Semin. Immunol.* **2014**, *26*, 253–266. [CrossRef]
4. Bhoj, V.G.; Chen, Z.J. Ubiquitylation in innate and adaptive immunity. *Nature* **2009**, *458*, 430–437. [CrossRef]
5. Sasaki, K.; Iwai, K. Roles of linear ubiquitinylation, a crucial regulator of NF-κB and cell death, in the immune system. *Immunol. Rev.* **2015**, *266*, 175–189. [CrossRef]
6. Karin, M.; Greten, F.R. NF-κB: Linking inflammation and immunity to cancer development and progression. *Nat. Rev. Immunol.* **2005**, *5*, 749–759. [CrossRef]
7. Baud, V.; Karin, M. Is NF-κB a good target for cancer therapy? Hopes and pitfalls. *Nat. Rev. Drug. Discov.* **2009**, *8*, 33–40. [CrossRef]
8. Gooz, M. ADAM-17: The enzyme that does it all. *Crit. Rev. Biochem. Mol. Biol.* **2010**, *45*, 146–169. [CrossRef]
9. Scheller, J.; Chalaris, A.; Garbers, C.; Rose-John, S. ADAM17: A molecular switch to control inflammation and tissue regeneration. *Trends Immunol.* **2011**, *32*, 380–387. [CrossRef]
10. Díaz-Rodríguez, E.; Montero, J.C.; Esparís-Ogando, A.; Yuste, L.; Pandiella, A. Extracellular signal-regulated kinase phosphorylates tumor necrosis factor-α-converting enzyme at threonine 735: A potential role in regulated shedding. *Mol. Biol. Cell* **2002**, *13*, 2031–2044. [CrossRef]
11. Soond, S.M.; Everson, B.; Riches, D.W.H.; Murphy, G. ERK-mediated phosphorylation of Thr735 in TNFα-converting enzyme and its potential role in TACE protein trafficking. *J. Cell Sci.* **2005**, *118*, 2371–2380. [CrossRef] [PubMed]
12. Liu, C.; Xu, P.; Lamouille, S.; Xu, J.; Derynck, R. TACE-mediated ectodomain shedding of the type I TGF-β receptor downregulates TNF-β signaling. *Mol. Cell* **2009**, *35*, 26–36. [CrossRef] [PubMed]

13. Xu, P.; Derynck, R. Direct activation of TACE-mediated ectodomain shedding by p38 MAP kinase regulates EGF receptor-dependent cell proliferation. *Mol. Cell* **2010**, *37*, 551–566. [CrossRef]
14. Kataoka, T. Chemical Biology of inflammatory cytokine signaling. *J. Antibiot.* **2009**, *62*, 655–667. [CrossRef]
15. Kataoka, T. Translation inhibitors and their unique biological properties. *Eur. J. Pharmacol.* **2012**, *676*, 1–5. [CrossRef] [PubMed]
16. Ogura, H.; Tsukumo, Y.; Sugimoto, H.; Igarashi, M.; Nagai, K.; Kataoka, T. Ectodomain shedding of TNF receptor 1 induced by protein synthesis inhibitors regulates TNF-α-mediated activation of NF-κB and caspase-8. *Exp. Cell Res.* **2008**, *314*, 1406–1414. [CrossRef]
17. Ogura, H.; Tsukumo, Y.; Sugimoto, H.; Igarashi, M.; Nagai, K.; Kataoka, T. ERK and p38 MAP kinase are involved in downregulation of cell surface TNF receptor 1 induced by acetoxycycloheximide. *Inter. Immunopharmacol.* **2008**, *8*, 922–926. [CrossRef]
18. Yamada, Y.; Taketani, S.; Osada, H.; Kataoka, T. Cytotrienin A, a translation inhibitor that induces ectodomain shedding of TNF receptor 1 via activation of ERK and p38 MAP kinase. *Eur. J. Pharmacol.* **2011**, *667*, 113–119. [CrossRef]
19. Hirano, S.; Kataoka, T. Deoxynivalenol induces ectodomain shedding of TNF receptor 1 and thereby inhibits the TNF-α-induced NF-κB signaling pathway. *Eur. J. Pharmacol.* **2013**, *701*, 144–151. [CrossRef]
20. Hirano, S.; Quach, H.T.; Watanabe, T.; Kanoh, N.; Iwabuchi, Y.; Usui, T.; Kataoka, T. Irciniastatin A, a pederin-type translation inhibitor, promotes ectodomain shedding of cell-surface tumor necrosis factor receptor 1. *J. Antibiot.* **2015**, *68*, 417–420. [CrossRef]
21. Quach, H.T.; Hirano, S.; Fukuhara, S.; Watanabe, T.; Kanoh, N.; Iwabuchi, Y.; Usui, T.; Kataoka, T. Irciniastatin A induces potent and sustained activation of extracellular signal-regulated kinase and thereby promotes ectodomain shedding of tumor necrosis factor receptor 1 in human lung carcinoma A549 cells. *Biol. Pharm. Bull.* **2015**, *38*, 941–946. [CrossRef]
22. Rozmer, Z.; Perjési, P. Naturally occurring chalcones and their biological activities. *Phytochem. Rev.* **2016**, *15*, 87–120. [CrossRef]
23. Wahab, H.A.; Yusof, R.; Rahman, N.A. A search for vaccines and therapeutic for Dengue: A review. *Curr. Comput. Aided. Drug Des.* **2007**, *3*, 341–352. [CrossRef]
24. Zhang, E.-H.; Wang, R.-F.; Guo, S.-Z.; Lin, B. An update on antitumor activity of naturally occurring chalcones. *Evid. Based Complement. Alternat. Med.* **2013**, *2013*, 815621. [CrossRef]
25. Synchrová, A.; Koláriková, I.; Žemlička, M.; Šmejkal, K. Natural compounds with dual antimicrobial and anti-inflammatory effects. *Phytochem. Rev.* **2020**, *19*, 1471–1502. [CrossRef]
26. Hwang, J.-K.; Chung, J.-Y.; Baek, N.-I.; Park, J.-H. Isopanduratin A from *Kaempferia pandurata* as an active antibacterial agent against cariogenic *Streptococcus mutans*. *Inter. J. Antimicrob. Agents* **2004**, *23*, 377–381. [CrossRef]
27. Song, M.-S.; Shim, J.-S.; Gwon, S.-H.; Lee, C.-W.; Kim, H.-S.; Hwang, J.-K. Antibacterial activity of panduratin A and isopanduratin A isolated from *Kaempferia pandurata* Roxb. against Acne-causing microorganisms. *Food Sci. Biotechnol.* **2008**, *17*, 1357–1360.
28. Yoon, J.-H.; Shim, J.-S.; Cho, Y.; Baek, N.-I.; Lee, C.-W.; Kim, H.-S.; Hwang, J.-K. Depigmentation of melanocytes by isopandu-ratin A and 4-hydroxypanduratin A isolated from *Kaempferia Pandurata* Roxb. *Biol. Pharm. Bull.* **2007**, *30*, 2141–2145. [CrossRef]
29. Morikawa, T.; Funakoshi, K.; Ninomiya, K.; Yasuda, D.; Miyagawa, K.; Matsuda, H.; Yoshikawa, M. Medicinal foodstuffs. XXXIV. Structures of new prenylchalcones and prenylflavannones with TNF-α and aminopeptidase N inhibitory activities from *Bosenbergia rotunda*. *Chem. Pharm. Bull.* **2008**, *56*, 956–962. [CrossRef]
30. Chatsumpun, N.; Sritularak, B.; Likhitwitayawuid, K. New biflavonoids with α-glucosidase and pancreatic lipase inhibitory activities from *Bosenbergia rotunda*. *Molecules* **2017**, *22*, 1862. [CrossRef]
31. Nguyen, N.T.; Nguyen, M.T.T.; Nguyen, H.X.; Dang, P.H.; Dibwe, D.F.; Esumi, H.; Awale, S. Constituents of the rhizomes of *Boesenbergia pandurata* and their antiausterity activities against the PANC-1 human pancreatic cancer line. *J. Nat. Prod.* **2017**, *80*, 141–148. [CrossRef]
32. Win, N.N.; Awale, S.; Esumi, H.; Tezuka, Y.; Kadota, S. Bioactive secondary metabolites from *Boesenbergia pandurata* of Myanmar and their preferential cytotoxicity against human pancreatic cancer PANC-1 cell line in nutrient-deprived medium. *J. Nat. Prod.* **2007**, *70*, 1582–1587. [CrossRef]
33. Nguyen, S.T.; Do, N.M.; Tran, D.H.-K.; To, N.B.; Vo, P.H.; Nguyen, M.T.T.; Nguyen, N.T.; Nguyen, H.X.; Truong, K.D.; Pham, P.V. Isopanduratin A isolated from *Boesenbergia pandurata* reduces HepG2 hepatocellular carcinoma cell proliferation in both monolayer and three-dimensional cultures. *Av. Exp. Med. Biol.* **2020**, *3*, 131–143.
34. Tanigaki, R.; Takahashi, R.; Nguyen, M.T.T.; Nguyen, N.T.; Do, T.V.N.; Nguyen, H.X.; Kataoka, T. 4-Hydroxypanduratin A and isopanduratin A inhibit tumor necrosis factor α-stimulated gene expression and the nuclear factor κB-dependent signaling pathway in human lung adenocarcinoma A549 cells. *Biol. Pharm. Bull.* **2019**, *42*, 26–33. [CrossRef] [PubMed]
35. Yun, J.-M.; Kwon, H.; Hwang, J.-K. In vitro anti-inflammatory activity of panduratin A isolated from *Kaempferia pandurata* in RAW264.7 cells. *Planta Med.* **2003**, *69*, 1102–1108. [PubMed]
36. Cheah, S.-C.; Appleton, D.R.; Lee, S.-T.; Lam, M.-L.; Hadi, A.H.A.; Mustafa, M.R. Panduratin A inhibits the growth of A549 cells through induction of apoptosis and inhibition of NF-kappaB translocation. *Molecules* **2011**, *16*, 2583–2598. [CrossRef]
37. Cheah, S.-C.; Lai, S.-L.; Lee, S.-T.; Hadi, A.H.A.; Mustafa, M.R. Panduratin A, a possible inhibitor in metastasized A549 cells through inhibition of NF-kappaB translocation and chemoinvasion. *Molecules* **2013**, *18*, 8764–8778. [CrossRef] [PubMed]
38. Kim, H.; Kim, M.-B.; Kim, C.; Hwang, J.-K. Inhibitory effects of panduratin A on periodontitis-induced inflammation and osteoclastogenesis through inhibition of MAPK pathways *in vitro*. *J. Microbiol. Biotechnol.* **2018**, *28*, 190–198. [CrossRef]
39. Kondo, T.; Takeda, K.; Muko, R.; Ito, A.; Chang, Y.-C.; Magae, J.; Kataoka, T. 4-*O*-Methylascochlorin inhibits the prolyl hydroxylation of hypoxia-inducible factor-1α, which is attenuated by ascorbate. *J. Antibiot.* **2019**, *72*, 271–281. [CrossRef]

40. Baba, K.; Kuwada, S.; Nakao, A.; Li, X.; Okuda, N.; Nishida, A.; Mitsuda, S.; Fukuoka, N.; Kakeya, H.; Kataoka, T. Different localization of lysosomal-associated membrane protein 1 (LAMP1) in mammalian cultured cell lines. *Histochem. Cell Biol.* **2020**, *153*, 199–213. [CrossRef]
41. Mitsuda, S.; Yokomichi, T.; Yokoigawa, J.; Kataoka, T. Ursolic acid, a natural pentacyclic triterpenoid, inhibits intracellular trafficking of proteins and induces accumulation of intercellular adhesion molecule-1 linked to high-mannose-type glycans in the endoplasmic reticulum. *FEBS Open Bio.* **2014**, *4*, 229–239. [CrossRef] [PubMed]
42. Quach, H.T.; Tanigaki, R.; Yokoigawa, J.; Yamada, Y.; Niwa, M.; Hirano, S.; Shiono, Y.; Kimura, K.; Kataoka, T. Allantopyrone A interferes with multiple components of the TNF receptor 1 complex and blocks RIP1 modifications in the TNF-α-induced signaling pathway. *J. Antibiot.* **2017**, *70*, 929–936. [CrossRef]
43. Vo, N.T.; Sasaki, S.; Miyake, Y.; Nguyen, N.T.; Dang, P.H.; Nguyen, M.T.T.; Kataoka, T. α-Conidendrin inhibits the expression of intercellular adhesion molecule-1 induced by tumor necrosis factor-α in human lung adenocarcinoma A549 cells. *Eur. J. Pharmacol.* **2021**, *890*, 173651. [CrossRef] [PubMed]
44. Shiono, Y.; Yokoi, M.; Koseki, T.; Murayama, T.; Aburai, N.; Kimura, K. Allantopyrone A, a new α-pyrone metabolite with potent cytotoxicity from an endophytic fungus, *Allantophomopsis Lycopodina* KS-97. *J. Antibiot.* **2010**, *63*, 251–253. [CrossRef]
45. Sonenberg, N.; Hinnebusch, A.G. Regulation of translation initiation in eukaryotes: Mechanisms and biological targets. *Cell* **2009**, *136*, 731–745. [CrossRef] [PubMed]
46. Merrick, W.C.; Pavitt, G.D. Protein synthesis initiation in eukaryotic cells. *Cold Spring Harb. Perspect. Biol.* **2018**, *10*, a033092. [CrossRef]
47. Yun, J.-M.; Kwon, H.; Mukhtar, H.; Hwang, J.-K. Induction of apoptosis by panduratin A isolated from *Kaempferia pandurata* in human colon cancer HT-29 cells. *Planta Med.* **2005**, *71*, 501–507. [CrossRef] [PubMed]
48. Yun, J.-M.; Kweon, M.-H.; Kwon, H.; Hwang, J.-K.; Mukhtar, H. Induction of apoptosis and cell cycle arrest by a chalcone panduratin A isolated from *Kaempferia pandurata* in androgen-independent human prostate cancer cells PC3 and DU145. *Carcinogenesis* **2006**, *27*, 1454–1464. [CrossRef]
49. Vanlangenakker, N.; Bertrand, M.J.M.; Bogaert, P.; Vandenabeele, P.; Vanden Berghe, T. TNF-induced necroptosis in L929 cells is tightly regulated by multiple TNFR1 complex I and II members. *Cell Death Dis.* **2011**, *2*, e230. [CrossRef]
50. Sa, B.-K.; Kim, C.; Kim, M.-B.; Hwang, J.-K. Panduratin A prevents tumor necrosis factor-alpha induced muscle atrophy in L6 rat skeletal muscle cells. *J. Med. Food* **2017**, *20*, 1047–1054. [CrossRef]
51. Aggarwal, B.B. Signalling pathways of the TNF superfamily: A double-edged sword. *Nat. Rev. Immunol.* **2003**, *3*, 745–756. [CrossRef]
52. Seals, D.F.; Courtneidge, S.A. The ADAMs family of metalloproteases: Multidomain proteins with multiple functions. *Genes Dev.* **2003**, *17*, 7–30. [CrossRef] [PubMed]
53. Donnelly, N.; Gorman, A.M.; Gupta, S.; Samali, A. The eIF2α kinases: Their structures and functions. *Cell. Mol. Life Sci.* **2013**, *70*, 3493–3511. [CrossRef] [PubMed]
54. Pakos-Zebrucka, K.; Koryga, I.; Mnich, K.; Ljujic, M.; Samali, A.; Gorman, A.M. The integrated stress response. *EMBO Rep.* **2016**, *17*, 1374–1395. [CrossRef] [PubMed]
55. Lai, S.-L.; Wong, P.-F.; Lim, T.-K.; Lin, Q.; Mustafa, M.R. Cytotoxic mechanisms of panduratin A on A375 melanoma cells: A quantitative and temporal proteomics analysis. *Proteomics* **2015**, *15*, 1608–1621. [CrossRef] [PubMed]
56. Pestka, J.J.; Zhou, H.-R.; Moon, Y.; Chung, Y.J. Cellular and molecular mechanisms for immune modulation by deoxynivalenol and other trichothecenes: Unraveling a paradox. *Toxicol. Lett.* **2004**, *153*, 61–73. [CrossRef]
57. Pestka, J.J. Mechanisms of deoxynivalenol-induced gene expression and apoptosis. *Food Addit. Contam. Part A Chem. Anal. Control. Expo. Risk Assess.* **2008**, *25*, 1128–1140. [CrossRef]